Crystal structural analysis and metal-dependent stability and activity studies of the ColE7 endonuclease domain in complex with DNA/Zn2+ or inhibitor/Ni2+

Lyudmila G. Doudeva, Hsinchin Huang, Kuo-Chiang Hsia, Zhonghao Shi, Chia-Lung Li, Yongliang Shen, Yi-Sheng Cheng and Hanna S. Yuan

---

References	This article cites 41 articles, 12 of which can be accessed free at: **http://www.proteinscience.org/cgi/content/full/15/2/269#References**
Email alerting service	Receive free email alerts when new articles cite this article - sign up in the box at the top right corner of the article or **click here**

Notes

To subscribe to *Protein Science* go to:
http://www.proteinscience.org/subscriptions/

Crystal structural analysis and metal-dependent stability and activity studies of the ColE7 endonuclease domain in complex with DNA/Zn^{2+} or inhibitor/Ni^{2+}

LYUDMILA G. DOUDEVA,[1] HSINCHIN HUANG,[1,2] KUO-CHIANG HSIA,[1] ZHONGHAO SHI,[1] CHIA-LUNG LI,[1] YONGLIANG SHEN,[1,3] YI-SHENG CHENG,[1] AND HANNA S. YUAN[1,2,3]

[1]Institute of Molecular Biology, Academia Sinica, Taipei, Taiwan, Republic of China
[2]Institute of Biochemistry, National Yang-Ming University, Taipei, Taiwan, Republic of China
[3]Institute of Biochemistry and Molecular Biology, College of Medicine, National Taiwan University, Taipei, Taiwan, Republic of China

Abstract

The nuclease domain of ColE7 (N-ColE7) contains an H-N-H motif that folds in a $\beta\beta\alpha$-metal topology. Here we report the crystal structures of a Zn^{2+}-bound N-ColE7 (H545E mutant) in complex with a 12-bp duplex DNA and a Ni^{2+}-bound N-ColE7 in complex with the inhibitor Im7 at a resolution of 2.5 Å and 2.0 Å, respectively. Metal-dependent cleavage assays showed that N-ColE7 cleaves double-stranded DNA with a single metal ion cofactor, Ni^{2+}, Mg^{2+}, Mn^{2+}, and Zn^{2+}. ColE7 purified from *Escherichia coli* contains an endogenous zinc ion that was not replaced by Mg^{2+} at concentrations of < 25 mM, indicating that zinc is the physiologically relevant metal ion in N-ColE7 in host *E. coli*. In the crystal structure of N-ColE7/DNA complex, the zinc ion is directly coordinated to three histidines and the DNA scissile phosphate in a tetrahedral geometry. In contrast, Ni^{2+} is bound in N-ColE7 in two different modes, to four ligands (three histidines and one phosphate ion), or to five ligands with an additional water molecule. These data suggest that the divalent metal ion in the His-metal finger motif can be coordinated to six ligands, such as Mg^{2+} in I-PpoI, *Serratia* nuclease and Vvn, five ligands or four ligands, such as Ni^{2+} or Zn^{2+} in ColE7. Universally, the metal ion in the His-metal finger motif is bound to the DNA scissile phosphate and serves three roles during hydrolysis: polarization of the P–O bond for nucleophilic attack, stabilization of the phosphoanion transition state and stabilization of the cleaved product.

Keywords: Protein nucleic acid interactions; nonspecific nuclease; DNase; DNA hydrolysis mechanism; H-N-H motif; $\beta\beta\alpha$-metal motif; colicin E7

Nucleases are a group of enzymes not only capable of nucleic acid binding but also of hydrolyzing phosphodiester linkages. They were considered to play a digestive role in nucleic acid salvage pathways and detailed structural and functional characterizations of the DNA/RNA-digestion nucleases, such as RNase A (Raines 1998) and DNase I (Suck 1994), have been conducted extensively. These nonspecific nucleases usually contain a crescent-shaped structure that binds nucleic acid substrates with a concaved surface but they do not contain any of the specific nucleic acid-binding modules that are usually found in DNA-binding proteins, such as zinc fingers (Laity et al. 2001) and the HMG domain (Travers 2000). With regard to function, we now know that nucleases are also involved in many cellular processes, including DNA repair, replication, recombination, transposition, and topoisomerization, as well as RNA

processing, splicing, interference, and editing (Mishra 2002). However, with respect to structure, only a few motifs have been identified as being involved in nucleic acid binding and cleavage (Chevalier and Stoddard 2001). The $\beta\beta\alpha$-metal motif (or so-called His-metal finger) is one such structural module capable of both DNA binding and cleavage.

The $\beta\beta\alpha$-metal motif was initially identified based on a structural comparison between the endonuclease active sites in the site-specific homing endonuclease I-PpoI and the nonspecific endonucleases *Serratia* nuclease and ColE9/ColE7 (Friedhoff et al. 1999; Kuhlmann et al. 1999). A structural motif with topology similar to that of a zinc finger, containing two antiparallel β-strands and one α-helix with a centrally bound divalent metal ion, was identified in these endonucleases, even though they shared little sequence homology. Subsequently, this motif was identified in a structural-specific endonuclease, phage T4 Endo VII (Raaijmakers et al. 1999), and a periplasmic nonspecific nuclease Vvn (Li et al. 2003) from *Vibrio vulnificus*. An alkaline metal ion, usually Mg^{2+}, is often bound in the $\beta\beta\alpha$-metal motif of most of these endonucleases, including I-PpoI (Galburt et al. 1999), *Serratia* nuclease (Miller et al. 1999), and Vvn (Li et al. 2003). A general single metal ion mechanism has been suggested, in which the scissile phosphate is directly bound and stabilized by the Mg^{2+} ion; a histidine functions as the general base to activate a water molecule for the nucleophilic attack to the scissile phosphate; a Mg^{2+}-bound water molecule provides a proton to the 3′-oxygen leaving group (Galburt et al. 1999; Miller et al. 1999; Li et al. 2003). In addition to alkaline earth metal ions, transition metal ions have also been identified in $\beta\beta\alpha$-metal motifs, including Ni^{2+} in ColE9 (Kleanthous et al. 1999) and Zn^{2+} in ColE7 (Ko et al. 1999). However, it is not known how these transition metal ion-bound $\beta\beta\alpha$-metal motifs participate in DNA hydrolysis, since a Mg^{2+} prefers to coordinate to "hard" oxygen-donor atoms but Zn^{2+} is usually coordinated not only to oxygen but also to the "softer" nitrogen- and sulfur-donor atoms (Dudev and Lim 2003). Hence, the numbers of metal-bound water molecules and amino acids coordinated to these metal ions differ.

This study used ColE7 to decipher how transition metal ions are bound in $\beta\beta\alpha$-metal motifs and how a Zn-bound ColE7 binds DNA nonspecifically. ColE7 is an *Escherichia coli* released toxin that contains three functional domains: receptor-binding, translocation, and nuclease (Hsia et al. 2005). After import into the target cell with the help of its receptor-binding and translocation domains, the nuclease domain of ColE7 (refer to N-ColE7 hereafter) digests chromosomal DNA to kill the foreign cell (Ku et al. 2002). N-ColE7 contains an H-N-H motif, identified originally from a subfamily of homing endonucleases (Gorbalenya 1994; Shub et al. 1994). Crystal structures of zinc-bound N-ColE7 in complex with an inhibitor Im7 protein (Chak et al. 1996) or a phosphate ion (Cheng et al. 2002) have shown that the H-N-H motif folds into a $\beta\beta\alpha$-metal topology with the zinc ion bound to three histidine side chains and a water molecule (or a phosphate ion) in a tetrahedral geometry. The apo-N-ColE7 only binds but cannot cleave dsDNA but the zinc-bound N-ColE7 binds and cleaves dsDNA (Ku et al. 2002). Moreover, wild-type N-ColE7 has been cocrystallized with an 8-bp palindromic duplex DNA (5′-GCGATCGC-3′) in the absence of a divalent metal ion, the structure of which showed for the first time the minor-groove binding and nonspecific interactions between an H-N-H endonuclease and DNA duplex (Hsia et al. 2004).

The metal ion-dependent activities of nuclease-type colicins have been controversial ever since a homologous ColE9 protein was shown to contain endonuclease activity with Ni^{2+} or Mg^{2+}, but not with Zn^{2+} (Pommer et al. 1999, 2001). The crystal structure of a mutated nuclease domain of ColE9 in complex with an 8-bp duplex DNA in the presence of a zinc ion showed that Zn^{2+} was bound to three conserved histidines and the scissile phosphate (Mate and Kleanthous 2004). It was suggested that because the zinc ion had no metal-bound water molecule, the zinc-bound ColE9 was not an active endonuclease. However, recently a study in single-stranded DNA cleavage by ColE7 and ColE9 using electrospray ionization mass spectrometry showed that whereas ColE9 is not active with Zn^{2+} and Mg^{2+} and only active with Ni^{2+} and Co^{2+}, ColE7 is active with Zn^{2+} and Ni^{2+} (van den Heuvel et al. 2005). This result shows that although nuclease colicins share high sequence identity (~65%), the metal ion cofactors, including Zn^{2+}, Ni^{2+}, and Mg^{2+}, coactivate each endonulease not necessarily in the same way. Moreover, the roles of transition and alkaline metal ions in His-metal finger endonucleases remain elusive.

Here, to further confirm and clarify the binding modes of transition metal ions and the respective metal-mediated nuclease activities in $\beta\beta\alpha$-metal endonucleases, we measured the metal ion-dependent activity of ColE7 and cocrystallized a mutated N-ColE7 with a 12-bp duplex DNA in the presence of zinc ions. The Zn^{2+} ion in the N-ColE7/DNA complex is bound tetrahedrally to three histidine residues and the scissile phosphate. Based on the results of melting point assays for the zinc-bound N-ColE7 in various concentrations of Mg^{2+}, we suggest that Zn^{2+} is the physiologically relevant metal ion used in *E. coli*. We also determined the crystal structure of a Ni-bound N-ColE7 in complex with the inhibitor Im7 in which the Ni^{2+} is bound in two different modes in

N-ColE7. The role of these four-, five-, or six-coordinated metal ions in the His-metal finger is discussed.

Results

ColE7 metal ion-dependent endonuclease activity

To determine the metal ion-dependent activity of ColE7, the metal ions originally associated with purified N-ColE7 were carefully removed by applying the enzyme first to Chelex 100 resin, followed by incubation with EDTA. The apo-enzyme was then dialyzed with four different high purity divalent metal ions, Zn^{2+}, Mn^{2+}, Ni^{2+}, and Mg^{2+}. The melting points of the apo- and metal ion-bound enzymes were then measured by circular dichroism (see Fig. 1A). The Zn- and Ni-enzymes had higher melting temperatures of $80.8 \pm 0.8°C$ and $80.8 \pm 1.4°C$, respectively compared to that of the apo-enzyme. In contrast, the Mg- and Mn-enzymes had melting temperatures of $75.5 \pm 0.1°C$ and $73.1 \pm 0.8°C$, similar to the melting point of the apo-enzyme ($74.3 \pm 0.7°C$). These results show that the transition metal ions, Zn^{2+} and Ni^{2+}, stabilize N-ColE7 better than Mn^{2+} and Mg^{2+}.

The endonuclease activities for the Zn-, Mn-, Ni-, and Mg-bound enzymes and apo-enzyme were assayed by plasmid digestion experiments using a supercoiled pQE-70 plasmid as the substrate. The resultant DNA digestion patterns are shown in Figure 2A. The apo-enzymes did not contain any residual endonuclease activity, showing that all the metal ions had been removed. The single-metal ion-bound (Zn^{2+}, Mn^{2+}, Ni^{2+}, and Mg^{2+}) N-ColE7 all contained endonuclease activity, in the order of $Ni^{2+} > Mn^{2+} \sim Mg^{2+} > Zn^{2+}$. This result shows that both transition metal ions (Ni^{2+}, Mn^{2+}, or Zn^{2+}) and an alkaline earth metal ion (Mg^{2+}) can function as cofactors to activate ColE7 endonuclease activity. This result agrees with our previous report showing that apo-N-ColE7 has no endonuclease activity and zinc-bound N-ColE7 is capable of digesting a 30-bp DNA (Ku et al. 2002).

The Mg-enzyme and Zn-enzyme were further incubated with a second metal ion (0.1–100 mM) to test if the second metal ion would enhance or inhibit endonuclease activity. The endonuclease activity of the Zn-enzyme and Mg-enzyme were enhanced by addition of 0.1–10 mM Mg^{2+} or 0.1–100 mM Zn^{2+}, but the activity was inhibited by addition of 100 mM Mg^{2+} (see Fig. 2B). This indicates that higher concentration of Mg^{2+} (in 100 mM range) inhibits the endonuclease activity of ColE7. The addition of Zn^{2+} up to 100 mM to N-ColE7 did not inhibit enzyme activity, in contrast to our previous observations (Ku et al. 2002). This is likely because an improved method is used here for apo-en-
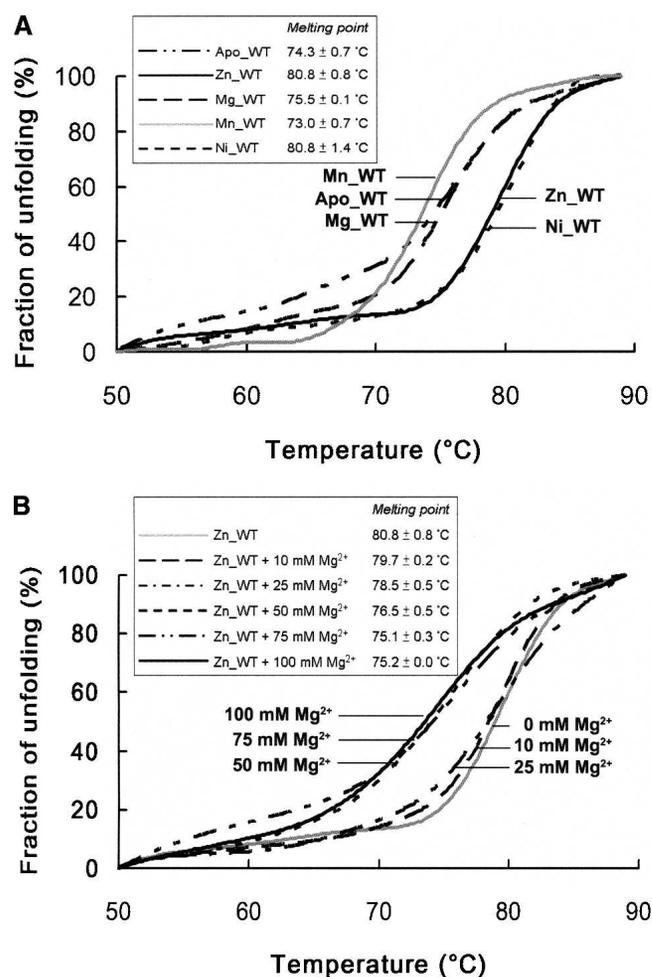
Figure 1. Measurements of the melting points for apo- and metal-bound N-ColE7 by circular dichroism. (*A*) The melting points of the apo- and each metal-bound N-ColE7 were measured by circular dichroism at a wavelength of 222 nm. The protein concentration used for all measurements was 0.1 mg/mL in 10 mM Tris-HCl (pH 8.0). The melting points were $74.3 \pm 0.7°C$ for apo-N-ColE7, $75.5 \pm 0.1°C$ for Mg-bound, $73.1 \pm 0.8°C$ for Mn-bound, $80.8 \pm 0.8°C$ for Zn-bound, and $80.8 \pm 1.4°C$ for Ni-bound N-ColE7. (*B*) The zinc-bound N-ColE7 was mixed with buffers containing 10–100 mM $MgCl_2$. The melting points of N-ColE7 in 10 and 25 mM Mg^{2+} buffers were ~80°C, close to that of the Zn-bound enzyme, indicating that zinc was still bound in N-ColE7. However, the melting points of N-ColE7 in 50, 75, and 100 mM Mg^{2+} buffers were shifted to ~75°C, indicating that Zn^{2+} was not bound to N-ColE7 when Mg^{2+} concentrations were > 50 mM.

zyme preparation, which produced protein sample with better quality than previous ones for biochemical assays (see Discussion).

Zn^{2+} versus Mg^{2+} binding in ColE7

Approaching this study, it was not certain whether ColE7 is bound to Zn^{2+} or Mg^{2+} in cells. Previously we
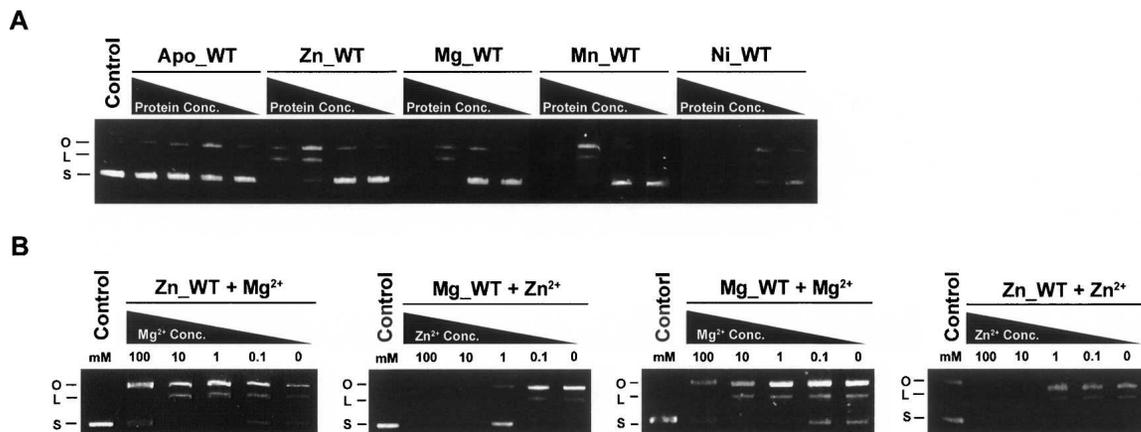
Figure 2. The metal-dependent endonuclease activity of N-ColE7 (the nuclease domain of ColE7). (*A*) The endonuclease activity of N-ColE7 was analyzed by plasmid digestion assays using pQE-70 as the substrate (see Control lane). Various amounts of apo-N-ColE7 (0.05, 0.27, 1.33, and 6.67 μM), did not cleave plasmids (100 ng). However, the endonuclease activity of apo-N-ColE7 was reactivated by the presence of one of the metal ions, Ni^{2+}, Mn^{2+}, Mg^{2+}, and Zn^{2+}. Ni-N-ColE7 cleaved plasmids at 0.05 μM; Mn- and Mg-N-ColE7 cleaved plasmids at 0.27 μM; and Zn-N-ColE7 cleaved plasmids at ~1.33 μM. (*B*) Different concentrations of Zn^{2+} and Mg^{2+} (0, 0.1, 1.0 10.0, 100.0 mM, as indicated in the figure) were added to Zn-bound and Mg-bound N-ColE7. Both Mg^{2+} (0.1 to 10 mM) and Zn^{2+} (0.1 to 100 mM) enhanced ColE7 endonuclease activity, but 100 mM of Mg^{2+}-inhibited enzyme activity. (O) Open, (L) linear, and (S) supercoiled DNA.

showed that N-ColE7 purified from *E. coli* contains endogenous Zn^{2+} based on atomic-emission measurements (Ko et al. 1999). To find out if this zinc ion in ColE7 could be replaced by Mg^{2+}, we measured the melting points of Zn-bound N-ColE7 in the presence of 10–100 mM $MgCl_2$. Since Zn-bound N-ColE7 has a higher melting point than that of Mg-bound N-ColE7, the melting point of the Zn-bound N-ColE7 should drop from ~80°C to ~75°C when Mg^{2+} replaced Zn^{2+}. Figure 1B shows that Zn^{2+} in N-ColE7 was not replaced by 10 and 25 mM Mg^{2+}. But when Mg^{2+} concentrations were >50 mM, Mg^{2+} replaced Zn^{2+} in ColE7, resulting in lower melting points for the enzyme. This result suggests that N-ColE7 is bound to Zn^{2+} in physiological conditions at which Mg^{2+} has a concentration of 1–2 mM in *E. coli* (Alatossava et al. 1985).

Abolished or reduced endonuclease activities in H545 or H573 mutants

Two highly conserved histidine residues in the H-N-H motif of N-ColE7 were mutated to generate five single-point mutants: H545A, H545E, H545Q, H573A, and H573E. Mutant enzymes were dialyzed in buffers containing zinc ion and the endonuclease activities of the zinc-bound mutants were assayed by plasmid digestion experiments in Tris-HCl buffers (pH 8.0). The H545 mutants H545A and H545E showed no endonuclease activity; however, H545Q still contained residual activity (see Fig. 3). H573A and H573E showed reduced enzyme activity as compared to that of wild-type N-ColE7. This result shows that H545 in N-ColE7 plays a critical role in DNA

hydrolysis. Similar results from ColE9 have reported that mutation of H103 (equivalent to H545 in ColE7) to alanine in ColE9 resulted in a mutant with no DNase activity in the presence of Ni^{2+} or Mg^{2+} (Walker et al. 2002). The two inactive N-ColE7 mutants, H545A and H545E, were then used for cocrystallization with DNA in the presence of metal ion cofactors to avoid DNA digestion by the enzyme during crystallization.

Crystal structure determination of H545E/DNA/Zn^{2+} complex

The H545E mutant was first dialyzed with a buffer containing EDTA followed by $ZnCl_2$ to ensure that the enzyme contained only Zn^{2+} ion. A 12-mer DNA with a palindromic sequence of 5′-CGGGATATCCCG-3′ was then successfully cocrystallized with the zinc-bound mutant enzyme. Similar procedures have been used to produce Ni-bound mutant proteins, which however did not cocrystallize with any of the tested DNA oligonucleotides. The H545E/DNA/Zn^{2+} ternary complex crystallized in a tetragonal space group $P4_12_12$, diffracting X-rays to a resolution of 2.5 Å. The structure was solved by molecular replacement using the crystal structure of N-ColE7 (PDB entry 7CEI) in the heterodimer of N-ColE7/Im7 as the search model. After model building and structural refinement for the enzyme and DNA molecules, the omit difference map ($F_o - F_c$) showed clearly the presence of a zinc ion with a peak of 12 σ in N-ColE7 (see Fig. 4A). Further positional and temperature factor refinements gave a reasonable tetragonal geometry and a B-factor of 34.7 Å^2 for the zinc ion. The electron density
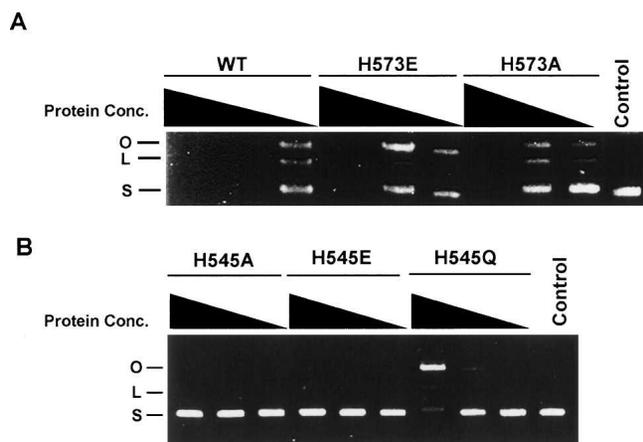
Figure 3. The endonuclease activities of N-ColE7 mutants analyzed by plasmid digestion assays. (*A*) Various amounts (0.01, 0.05, and 0.27 μM) of zinc-bound wild-type and mutated N-ColE7 were incubated with pQE-70 plasmids (100 ng) in 10 mM Tris-HCl (pH 8.0) for 20 min at 37°C. The digested DNA was resolved on 1% agarose gels. The wild-type N-ColE7 started to digest plasmids at 0.01 μM. The H573E and H573A N-ColE7 mutants showed reduced endonuclease activities, only starting to cleave DNA at ~0.05 μM. (*B*) The H545A and H545E mutants of N-ColE7 had no endonuclease activity when the enzyme concentration was increased from 0.01 to 0.27 μM. But H545Q mutant had residual endonuclease activity, cleaving DNA at ~0.27 μM. (O) Open, (L) linear, and (S) supercoiled DNA.

map for the loop between βd and βe, from residues 548 to 554, was ill defined and the structural model in this region was thus not built. The electron density in the rest of the region in N-ColE7 and DNA was well defined. The final R-factor/R_{free} is 24.0/28.7% for 7597 reflections. The final model contains one protein molecule (chain A: residues 450–547 and 555–574), one duplex DNA molecule (chain B/C), one zinc ion, and 33 water molecules. The diffraction and refinement statistics for the H545E/DNA/Zn^{2+} complex are listed in Table 1.

Overall structure of H545E/DNA/Zn^{2+} complex

The overall structure of H545E/DNA/Zn^{2+} complex in one asymmetric unit is shown in Figure 5A. The enzyme has a mixed α/β fold, containing an H-N-H motif (βd, βe, and α5) with a concave surface. The H545E enzyme structure in the complex was superimposed with that of the free form of N-ColE7 (PDB 1M08), inhibitor-bound N-ColE7 (PDB 7CEI), and octamer DNA-bound N-ColE7 (PDB 1PT3). The average RMS differences between Cα atoms were all <0.6 Å, indicating that the overall structure of N-ColE7 is quite rigid and not changed in the absence or presence of bound inhibitor or different DNA oligonucleotides.

The H-N-H motif is bound primarily to the minor groove of DNA in such a way that the α5-helix inserts into the minor groove with βd strand located next to the phosphate backbone. Apart from the H-N-H motif, the N-terminal end of the α2-helix also interacts with the neighboring DNA major groove. One of the sugar phosphate backbones in the DNA duplex is therefore clamped between the H-N-H motif and the α-2 helix. The zinc ion in the H-N-H motif is bound directly to the P5 phosphate in the 12-mer DNA.

A schematic diagram of the detailed contacts between H545E and a 12-mer DNA, including hydrogen bonds and van der Waals contacts, is shown in Figure 6A. As expected for a nonspecific nuclease, most of the contacts are between protein and DNA phosphate backbones. There are altogether 12 hydrogen bonds, ten bound to phosphates, one to sugar, and only one directly to the base (N6 of ADE7 bound to OD2 of D493). D493 in the apo-N-ColE7/8-mer DNA complex (PDB 1PT3) also forms a hydrogen bond with a non-adenine DNA base (N4 of CYT6 bound to OD2 of D493), indicating that this hydrogen bond contributes to protein–DNA binding affinity but not DNA specificity. This result again shows that the nonspecific N-ColE7 interacts with DNA primarily via phosphate backbones thus avoiding sequence-dependent interactions with DNA bases (Hsia et al. 2005).

Structure of the Zn-bound endonuclease active site

A detailed view of the ββα-metal motif of the endonuclease active site of the H545E/DNA/Zn^{2+} complex is shown in Figure 5B. The zinc ion is bound to the side chains of three histidines (H544, H569, and H573) and the scissile phosphate in a tetrahedral geometry. The omitting electron density for the substituted E545 was clearly visible, but the electron density of one of the zinc-bound histidine residues (H573) was not fully defined. Similar tetrahedral coordination around the zinc ion has been reported in the 2.4 Å structure of N-ColE9 (H103A mutant) in complex with an 8-mer DNA (Mate and Kleanthous 2004). The bond distances and angles surrounding Zn^{2+} are within a reasonable range (see Fig. 3A): 2.1 Å (Zn-$N_{\delta1}$/H544), 1.9 Å (Zn-$N_{\epsilon2}$/H569), 1.9 Å (Zn-$N_{\epsilon2}$/H573), and 2.1 Å (Zn-O/P4) with bond angles of between 102.4° to 117.4°.

To find out if there was any conformational difference between the apo- and holo-enzymes, the active site of the zinc-bound H545E/12-mer DNA complex was superimposed with that of the zinc-free wild-type N-ColE7/8-mer DNA (see Fig. 5B). Except for H573, which shifted slightly in the zinc-free structure, all of the other amino acid side chains, as well as the scissile phosphates, fitted well with each other. The major difference between the two structures was the long loop (residues 447 to 452) between the two β-strands that was visible in the wild-type enzyme but disordered in the H545E mutant. Since H545 is thought to function as the general base, the
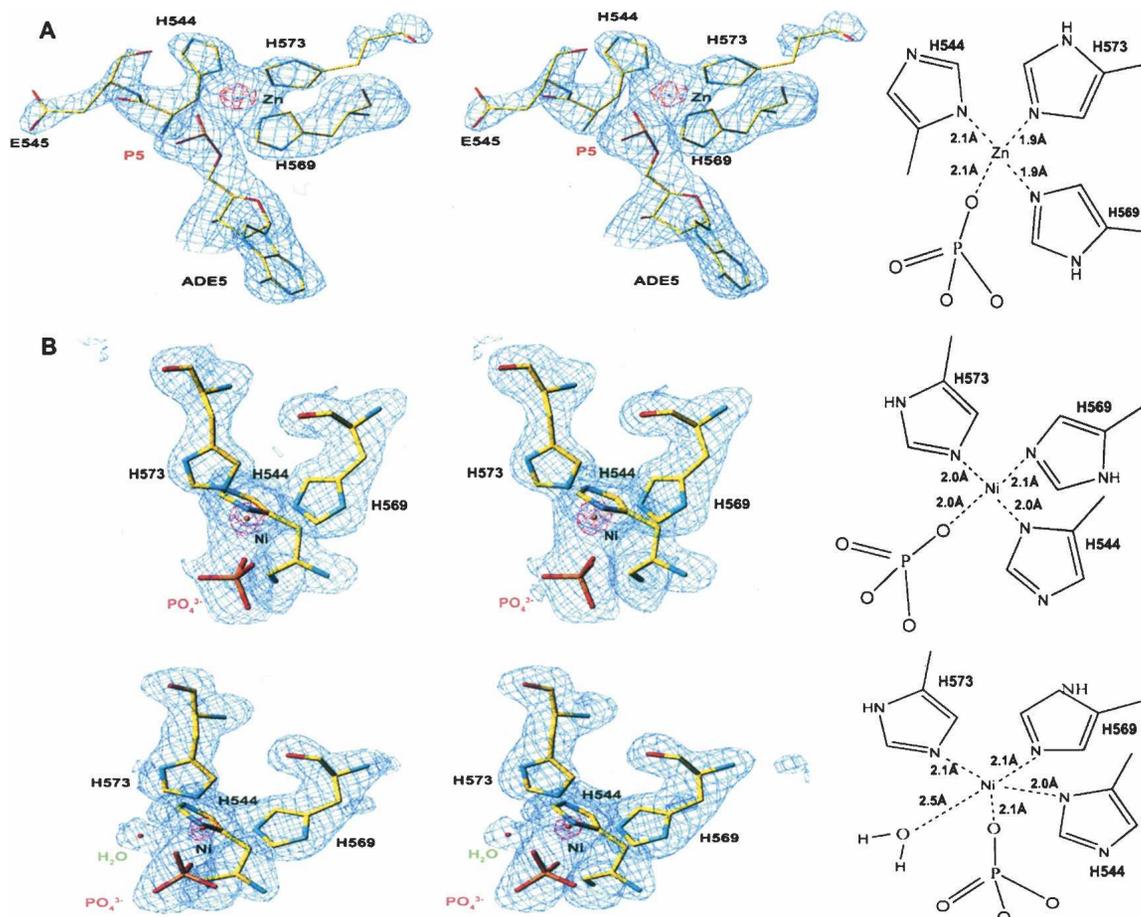
Figure 4. The omit electron density maps of Zn-bound and Ni-bound endonuclease active sites in H545E/DNA/Zn^{2+} and N-ColE7/Im7/Ni^{2+} complexes, respectively. (*A*) Stereo view of the omit difference maps ($F_o - F_c$) contoured at 2.5 σ (blue) and 12.0 σ (red) shows that the DNA scissile phosphate (P5) is bound directly to the zinc ion. The tetrahedral geometry and bond distances around the Zn atom are schematically shown in the *right* panel. (*B*) Stereo views of the omit difference maps contoured at 2.5 σ (blue) and 18.0 σ (red) around the Ni-binding site in the two noncrystallographic-symmetry related molecules in N-ColE7/Im7/Ni^{2+} complex structure. In molecule A, Ni^{2+} is bound to three histidines and a phosphate in a tetrahedral geometry. In molecule B, Ni^{2+} is bound to three histidines, a phosphate, and a water molecule in a distorted trigonal bi-pyramidal geometry.

replacement of H545 with glutamate destroyed the enzyme's activity. Accordingly, the nucleophilic water molecule supposedly associated with H545 was not visible in the mutant complex.

Crystal structure of Ni-bound N-ColE7/Im7

It has been reported that Ni^{2+} ion in ColE9, although bound at the same site in the H-N-H motif, is coordinated differently from the Zn^{2+} in ColE7, in that only two rather than three histidines are involved in metal binding (Kleanthous et al. 1999). It was proposed that the different metal ion coordination was critical for the metal-dependent activity (Keeble et al. 2002; Mate and Kleanthous 2004). We therefore further determined the crystal structure of Ni-bound N-ColE7/Im7 to reveal the Ni-binding mode in ColE7. The protein complex of

the mutated N-ColE7 (H545E) and Im7 was first dialyzed with EDTA to remove any associated metal ions. The EDTA-treated apo-protein was then dialyzed with $NiCl_2$ before crystallization. The Ni-bound N-ColE7/Im7 crystals were isomorphous to the Zn-bound N-ColE7/Im7 (PDB entry 1MZ8), diffracting X-rays to a resolution of 2.0 Å. There were two protein complexes per asymmetric unit and the final refinement statistics are listed in Table 1.

The final omit map surprisingly showed that the two Ni-binding sites in the two NCS-related ColE7 were different (see Fig. 4B). The molecule A contained a Ni^{2+} bound to three histidine residues (H544, H569, and H573) and one phosphate ion in a tetrahedral geometry, similar to that of the Zn-binding site revealed previously (Sui et al. 2002). The molecule B contained a Ni^{2+} bound to three histidines, one phosphate ion, and a water molecule in a distorted trigonal bi-pyramidal geometry. The bond

Table 1. *Data collection and refinement statistics*

	H545E /DNA/Zn^{2+}	N-ColE7 /Im7/Ni^{2+}
Data collection and processing		
Space group	$P4_12_12$	$P2_12_12$
Cell dimensions	a = 44.19 Å,	a = 119.02 Å
	b = 44.19 Å,	b = 62.88 Å,
	c = 203.97 Å	c = 74.77 Å
Resolution (Å)	2.5	2.0
Observed reflections	89,323	224,307
Unique reflections	7597	38,583
Completeness—all	98.0	99.8
data (%)	(50.0–2.5 Å)	(50.0–2.0 Å)
Completeness—last	99.5	99.9
shell (%)	(2.59–2.50 Å)	(2.07–2.00 Å)
R_{sym} —all data (%)[a]	4.5	8.2
R_{sym} —last shell (%)[a]	15.1	38.1
$I/\sigma(I)$, all data	41.0	25.3
$I/\sigma(I)$, last shell	10.8	5.7
Refinement		
Resolution range (Å)	50.0–2.5	50.0–2.0
Reflections	7446	37,511
Nonhydrogen atoms		
Protein	963	3,330
DNA	486	0
Solvent molecules	33	423
R-factor (%)[b]	24.0	18.8
R_{free} (%)	28.7	23.5
Model quality		
RMS deviations in		
Bond lengths (Å)	0.014	0.008
Bond angles (deg)	1.65	1.3
Average B-factor (Å^2)		
Protein atoms	38.9	31.2
DNA atoms	35.2	0
Solvent atoms	33.3	40.0
Ramachandran plot (%)		
Most favored	89.1	93.5
Additionally allowed	7.9	5.9
Generously allowed	3.0	0.6
Disallowed	0	0

[a] $R_{sym} = \Sigma_{hkl}\Sigma_i |I_i(hkl) - \langle I(hkl)\rangle| / I_i(hkl)$.
[b] R-factor $= \Sigma_{hkl} ||F_o(hkl)| - |F_c(hkl)|| / \Sigma_{hkl} F_o(hkl)$.

distances between Ni^{2+} and imidazole nitrogen atoms were all in a reasonable range from 2.0 to 2.1 Å, except that the Ni-water bond was longer with a bond distance of 2.5 Å (see each bond distance in Fig. 4). This result indicates that Ni^{2+} may bind to the H-N-H motif of ColE7 in two different ways, one with and one without a metal-bound water molecule.

Discussion

Protein–DNA interactions

N-ColE7 bound 12-bp duplex DNA at its minor and major grooves with a buried protein surface of 967 Å^2.

This buried protein interface value is lower than the average value of ~1600 Å^2 found in most protein–DNA complexes (Jones et al. 1999; Nadassy et al. 1999). Nevertheless, the lower interface is consistent with its higher K_m value of ~75 nM (data not shown). The H-N-H motif in N-ColE7 is bound at the minor groove of DNA such that it induces DNA to bend about 19° (calculated by Curve) away from the enzyme. Compared to the 3° and 17° bending angles observed in the apo-N-ColE7/8-mer DNA complexes (Hsia et al. 2004), the DNA bend in the 12-mer complex is greater probably because the longer of the DNA allows it to interact with N-ColE7 more extensively. This is supported by the extra interactions at the 5′-end in the DNA C-strand (see Fig. 6A) and the more-buried surface in the 12-mer (967 Å^2), as compared to the 8-mer (682 Å^2) structures. The DNA minor groove in the 12-mer complex is widened from 5.6 Å of an ideal straight B-DNA to ~9 Å (Fig. 6B). Although the DNA sequences and the bending angles calculated from the two complexes seem different, superposition of the two complexes show that the DNA conformation is similar (data not shown), indicating that the enzyme induces bound DNA to de-form in a similar manner, independent of its sequence.

Comparison with other site-specific or nonspecific nucleases containing similar $\beta\beta\alpha$-metal motifs (Friedhoff et al. 1999; Kuhlmann et al. 1999), including the Vvn/DNA (PDB 1OUP) (Li et al. 2003) and I-PpoI/DNA (PDB 1A74) (Flick et al. 1998) complexes, shows that all these endonucleases induce DNA to bend right before the cleavage site (see Fig. 6B). The minor groove width of DNA in all these complexes is widened to 8–10 Å by the $\beta\beta\alpha$-metal motif bound at the minor groove. The DNA oligonucleotides are always cleaved at the 3′-side of the widened minor groove. This might indicate how sequence-preference cleavage is carried out by these nonspecific endonucleases.

Zinc is the physiological metal ion in ColE7

Controversial results have been obtained for the metal-dependent activities of nuclease colicins. It has been reported that ColE2, ColE7 ColE8, and ColE9 were not active with Zn^{2+} in dsDNA cleavage (van den Bremer et al. 2004); ColE9 was not active with Zn^{2+} but only active with Ni^{2+}, Co^{2+}, and Mg^{2+} in dsDNA cleavage and with Ni^{2+} and Co^{2+} for ssDNA cleavage (Pommer et al. 1999, 2001; van den Bremer et al. 2002). On the contrary, our previous results showed that apo-ColE7 binds but does not cleave DNA and zinc-bound ColE7 cleaves dsDNA (Ku et al. 2002). Recently a study using electrospray ionization mass spectrometry to detect ssDNA cleavage by ColE7 and ColE9 showed that while ColE7 is active with Zn^{2+} and Ni^{2+}, ColE9
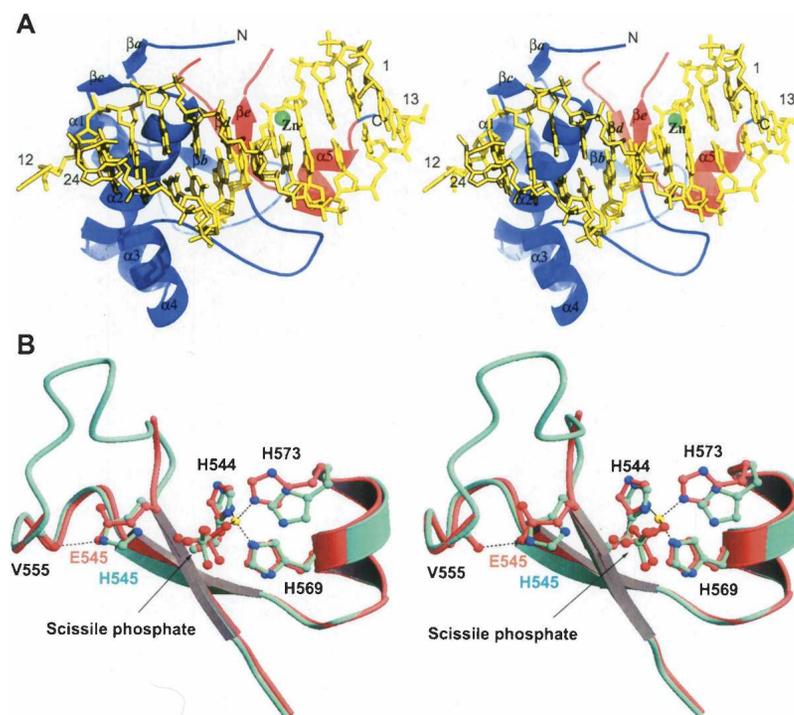
Figure 5. Stereo view of the H545E/DNA/Zn^{2+} crystal structure. (*A*) The H-N-H motif (red) of N-ColE7 (blue and red ribbon) is bound at the minor groove of DNA 12-mer (yellow). DNA is bent ~20° (calculated by Curve [Lavery and Sklenar 1988]) away from N-ColE7. The zinc ion (displayed as a green ball) is located closely to one of the phosphates in the DNA backbone. (*B*) The zinc-bound active site in the N-ColE7/12-mer DNA complex (red) was superimposed with the metal-free active site (green) in the N-ColE7/8-mer DNA complex (PDB entry 1PT3). The two structures fitted well with an average RMS difference of 0.34 Å for 18 C$_\alpha$ atoms located in β-strand or α-helix regions used for superimposition. In the zinc-bound active site, the zinc ion is coordinated to the side chains of H544, H569, and H573 and the scissile phosphate in a tetrahedral geometry. In the zinc-free active site, only H573 shifted away slightly. The loop between residues 548 to 554 was disordered and not modeled in the H545E/DNA/Zn complex.

is not active with Zn^{2+} and Mg^{2+} but only active with Ni^{2+} and Co^{2+} (van den Heuvel et al. 2005). This result shows that although endonuclease colicins share high sequence identity (~70%), the metal-dependent activities of these endonucleases are complicated issues even for in vitro analysis.

Although it would be interesting to find out which and why different metal ions are more efficient cofactors for nucleic acid (including ssDNA, dsDNA, and RNA) digestion, the key issue to be addressed at present is probably determining which metal ion is the physiological cofactor for ColE7. This depends on not only the metal-dependent enzyme activity but also the enzyme's metal-binding affinity and metallochaperones' specificity (Tottey et al. 2005). The endonuclease colicins have been shown to bind to Zn^{2+} most tightly (van den Bremer et al. 2004). ColE9 binds to Zn^{2+} with an estimated K$_d$ of less than nM range, while it binds to Ni^{2+} and Co^{2+} with K$_d$ in the μM range as measured by isothermal titration calorimetry, and it binds to Mg^{2+} much more weakly (Pommer et al. 1999). However, the cellular concentration of free Mg^{2+}, 1–2 mM

(Alatossava et al. 1985), is much higher than that of Zn^{2+}. Whereas the cellular zinc quota is millimolar, the free Zn^{2+} in cytoplasm has been estimated to be in femtomolar range, that is, less than one Zn^{2+} atom per bacterial cell (Outten and O'Halloran 2001). It is suggested that the newly synthesized zinc-requiring proteins acquire their Zn^{2+} from metallochaperones or zinc-buffering proteins (Blindauer and Sandler 2005; Tottey et al. 2005). Therefore, it would be informative to find out which metal ion is acquired in the protein in vivo.

Previously we found that ColE7 purified from *E. coli* contains endogenous Zn^{2+} by atomic emission and mass spectrometry studies (Ko et al. 1999), suggesting that Zn^{2+} is the metal ion bound with ColE7 in host cells. In this study, we observed that zinc-bound N-ColE7 has a higher melting point (~80°C) than that of apo- or magnesium-bound enzymes (~75°C) by CD measurements. The melting points measured here were much higher than the values reported previously, in which the apo-N-ColE7 had a melting point of 26.3°C and Zn-bound N-ColE7 had a melting point of 59.9°C as
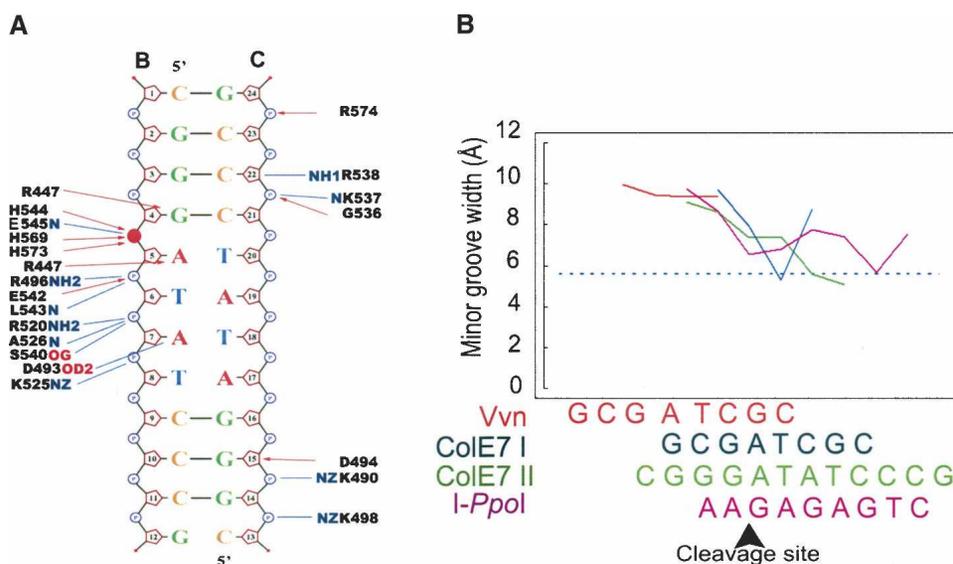
Figure 6. Schematic presentations of the interactions between N-ColE7 and DNA. (*A*) The solid blue lines indicate hydrogen bonds or salt bridges (<3.50 Å) and the red arrows show van der Waals contacts (<3.35 Å) between N-ColE7 and DNA. Most of the interactions are between proteins side chains and DNA phosphate backbones. (*B*) DNA groove widths were plotted for each base step in H545E/12-mer DNA complex (this study), N-ColE7/8-mer DNA complex (PDB entry 1PT3), Vvn/DNA (PDB entry 1OUP), and I-PpoI/DNA (PDB entry 1A74). The DNA cleavage sites are aligned and marked by a solid arrow, shown at the *bottom* of the figure. The minor groove widths are widened to ~9 Å at the region bound to ββα-metal motif in all complexes. DNA is cleaved right at the 3′-side of the widened minor groove.

measured by differential scanning calorimetry (van den Bremer et al. 2002). This difference may result from the different conditions used for melting point measurements, as well as the different methods of protein sample preparation used in the two studied. In this study, we improved the method and obtained a more stable apo-enzyme by applying the enzyme to a Chelex 100 resin followed by dialysis in buffers containing EDTA. We found that Zn^{2+} in N-ColE7 was not replaced by <25 mM Mg^{2+}, indicating that Zn^{2+} remained bound to ColE7 in cytoplasm where free Mg^{2+} concentration is 1–2 mM in *E. coli* (Alatossava et al. 1985). So based on four lines of evidence: (1) ColE7 acquires Zn^{2+} from *E. coli* cells; (2) nuclease colicins bind to Zn^{2+} most tightly; (3) the Zn^{2+} bound in ColE7 cannot be replaced by Mg^{2+} <25 mM; and (4) the virtue of the metal-associated residues (three softer histidines rather than harder oxygen-containing residues), we suggest that the transition metal ion, zinc, is the physiologically relevant metal ion for ColE7 in host *E. coli* cells.

Two different transition metal ion binding modes in N-ColE7

Most endonucleases bearing a ββα-metal fold active site, such as Vvn (Li et al. 2003) and I-PpoI (Galburt et al. 1999), cleave DNA via a Mg^{2+}-mediated single metal ion catalyzed mechanism. In Vvn (Flick et al. 1998) and I-PpoI (Galburt et al. 1999), Mg^{2+} (or

Ca^{2+}) ion is bound to one or two amino acid residues (asparagine and glutamate), a DNA scissile phosphate, and three or four water molecules in a six-coordinated octahedral geometry. One of the Mg^{2+}-bound water molecules plays a crucial role in donating a proton to the leaving 3′-oxygen group. In this study we confirm that the Zn^{2+} in ColE7 is coordinated to three amino acid residues (H545, H569, and H573) and the scissile phosphate in a tetrahedral geometry without any metal-bound water molecule. We have shown previously that Mn^{2+} is also bound in a tetrahedral geometry in ColE7 (Sui et al. 2002), similar to that of the zinc ion in ColE7.

We further show that Ni^{2+} can be bound with four ligands (three histidines and one phosphate) or with five ligands (three histidines, one phosphate, and one water molecule) in the crystal structure of N-ColE7/Im7/Ni^{2+}. The two different Ni^{2+} binding modes observed here indicate that Ni^{2+} could be bound with four or five coordination numbers equally well. N-ColE7 cleaves double-stranded DNA most efficiently with Mg^{2+} and Ni^{2+} and less efficiently with Zn^{2+} and Mn^{2+}. It seems to imply that the divalent metal ions bound with more waters in the His-metal finger are better cofactors for DNA hydrolysis. In comparison to other metal finger endonucleases, it has been shown that I-PpoI is most efficient in the presence of an oxophilic metal ion that prefers an octahedral geometry: $Mg^{2+} > Mn^{2+} > Ca^{2+} = Co^{2+} > Ni^{2+} > Zn^{2+}$ (Wittmayer and Raines 1996). The H-N-H homing endonuclease I-HmuI is also bound with a six-coordinated

metal ion and prefers Mg^{2+} and Mn^{2+} over Co^{2+}, Zn^{2+}, Ca^{2+}, and Sr^{2+} (Shen et al. 2004). However, the residues responsible for metal ion binding in these homing endonucleases all contain "hard" oxygen-donor atoms, Asn119 in I-PpoI, Asp74 and Asn96 in I-HmuI. We may therefore conclude that the metal finger endonucleases containing oxygen-donor residues for metal ion binding, such as I-PpoI, I-HmuI, Vvn, and *Serratia* nuclease, prefer a cofactor of Mg^{2+} bound in an octahedral geometry for DNA hydrolysis. However, bacterial colicins belong to a different subclass of metal finger endonucleases whose amino acid residues responsible for metal ion binding are "softer" histidines, therefore they prefer Zn^{2+} bound in a tetrahedral geometry. It remains unclear without the metal-bound water molecule functioning as the proton donor, how Zn-bound or Mn-bound ColE7 hydrolyze nucleic acid molecules. More studies are necessary to further clarify the DNA hydrolysis mechanism mediated by transition metal ion-bound metal finger endonucleases in the future.

In conclusion, we suggest that a transition metal ion may also be a cofactor for endonucleases containing a $\beta\beta\alpha$-metal fold active site. We also suggest that the zinc ion is the physiological relevant metal ion bound in ColE7 in host *E. coli*. The mutagenesis studies and the crystal structure of N-ColE7/DNA/Zn^{2+} ternary complex confirms that a strictly conserved histidine (His545 in ColE7) functions as the general base to activate a water molecule for nucleophilic attack to the scissile phosphate. The divalent metal ion binding to the scissile phosphate may serve three roles: polarization of the P-O bond for nucleophilic attack, stabilization of the phospho-anion transition state and stabilization of the cleaved product.

Materials and methods

Cloning, expression, and protein purification

Wild-type N-ColE7 and Im7 proteins were expressed using the vector pQE-70 (Qiagen), containing a 6-histidine affinity tag at the C terminus of the cloning site in *E. coli* M15 (Sui et al. 2002). Cells were incubated in LB medium at 37°C and induced by IPTG for 4 h once the $A_{600\ nm}$ reached 0.6 O.D. Crude cell extracts were loaded onto a Ni-NTA resin affinity column (Qiagen) and the bound protein was then eluted by an imidazole gradient solution. The eluent was dialyzed against 20 mM glycine-HCl buffer (pH 3.0) overnight to denature the protein complex. The resulting protein solution was loaded onto a Sepharose-SP column (HiTrap SP, Pharmacia) previously equilibrated with 20 mM glycine-HCl buffer (pH 3.0). The N-ColE7 was eluted by a NaCl gradient (pH 3.0) and Im7 was eluted afterward by a 20 mM sodium phosphate buffer (pH 7.0). The eluent containing N-ColE7 was dialyzed against 20 mM sodium phosphate buffer (pH 7.0) and then applied to a heparin column (HiTrap SP, Pharmacia). The free N-ColE7 containing residues 444–576 was then eluted by a NaCl gradient and dialyzed against 50 mM Tris-HCl (pH 7.5).

Each N-ColE7 mutant, including H545A, H545E, H545Q, H573E, and H573A, was constructed using a QuickChange site-directed mutagenesis kit (Stratagene) and was expressed and purified in the same manner as that of wild-typed N-ColE7. The molecular mass of each mutant measured by mass spectroscopy was 15,667 (calculated weight, 15664.8) for H545A; 15,725 (calculated weight, 15722.8) for H545E; 15,724 (calculated weight, 15721.0) for H545Q; 15,667 (calculated weight, 15664.7) for H573A; and 15722 (calculated weight, 15722.8) for H573E.

Endonuclease activity assay

The apo-enzyme without any metal ion cofactor was prepared by applying the N-ColE7 to Chelex 100 resin (Bio-Rad). The N-ColE7 was then eluted with a buffer containing 100 mM NaCl, 10 mM Tris-HCl (pH 8.0). The concentrated N-ColE7 (~1 mg/mL) was further incubated with 10 mM divalent metal chelating agent EDTA at 4°C overnight. The EDTA-treated N-ColE7 was dialyzed against 10 mM Tris-HCl buffer (pH 8.0) four times to remove any residual EDTA.

The metal-free N-ColE7 was dialyzed against four different buffers containing respectively 1 mM $ZnCl_2$ (99.999%), 1 mM $MnCl_2$ (99.99%), 1 mM $MgCl_2$ (99.995%) or 1 mM $NiCl_2(H_2O)_6$ (99.9999%), in 10 mM Tris-HCl (pH 8.0) at 4°C overnight (metal ion chloride compounds were from Sigma-Aldrich). The metal-treated N-ColE7 was then dialyzed against 10 mM Tris-HCl buffer (pH 8.0) with four changes of buffer independently. After dialysis, the single-metal ion-bound enzyme was obtained, i.e., Zn^{2+}-, Mn^{2+}-, Mg^{2+}-, and Ni^{2+}-bound N-ColE7, respectively.

Protein concentrations of the apo-N-ColE7, Zn^{2+}-N-ColE7, Mn^{2+}-N-ColE7, Mg^{2+}-N-ColE7, Ni^{2+}-N-ColE7 and all mutants were adjusted between 200 µg/mL and 1.6 µg/mL by series dilution. A supercoiled pQE-70 plasmid (100 ng) was used as the substrate for cleavage reactions throughout the experiments. The plasmid digestion experiment was performed for 20 min in 10 mM Tris-HCl (pH 8.0) at 37°C. The digested plasmids were analyzed by electrophoresis on 1% agarose gel. The nuclease activity of H545 and H573 mutants was measured by plasmid digestions as well in 10 mM Tris-HCl (pH 8.0).

CD measurement

The melting point of each protein sample was measured by circular dichroism at least three times. Thermal denaturation experiments were performed in 10-mm cuvettes at a wavelength of 222 nm on a Jasco J720 spectropolarimeter. The protein concentration used for all measurements was 0.1 mg/mL in 10 mM Tris-HCl (pH 8.0). The temperature was increased from 25°C to 95°C at a rate of 50°C/h. The transition curve (T_m) was fitted to a two-state unfolding model.

H545E/DNA/Zn^{2+} crystallization and data collection

Crystals of H545E/DNA/Zn^{2+} were obtained by the hanging drop vapor-diffusion method. A drop containing 10 mg/mL of the zinc-bound H545E N-ColE7, the equal molar ratio of the double-stranded DNA (5′-CGGGATATCCCG-3′), 25 mM Tris-HCl (pH 7.5), 0.1 M ammonium chloride, and 5.25% MPD was set against a reservoir of 0.2 M ammonium chloride

and 10.5% MPD. Plates of crystals appeared within several days at room temperature. X-ray diffraction intensities were collected at −150°C from an R-AXIS-IV++ imaging plate equipped with a double-mirror focusing system mounted on a rotating anode X-ray generator (MSC Co.). The H545E/DNA/Zn^{2+} crystallized in a tetragonal $P4_12_12$ space group with one protein and one DNA duplex per asymmetric unit. Cell parameters and diffraction statistics are listed in Table 1.

H545E/DNA/Zn^{2+} structure determination and refinement

The crystal structure of H545E/DNA/Zn^{2+} complex was determined by molecular replacement using the structure of N-ColE7 (PDB accession no. 7CEI) as the search model by the program CNS (Brunger et al. 1998). One obvious rotational and translational solution was identified and subsequent structural refinement was carried out by the program CNS, with 8% of data selected randomly and set aside for calculation of R_{free} values. After positional and B-factor refinement of the protein molecule, the Fourier maps gave a clear continuous electron density for the 12-mer and the DNA structural model was built accordingly. The final protein–DNA complex model had an R-factor of 24.0% and an R_{free} of 28.7% for 7597 reflections in the resolution range of 50.0–2.5 Å. Structural coordinates and diffraction structure factors have been deposited in the Protein Data Bank with a PDB ID code of 1ZNS or a RCSB ID code of RCSB032932. The final refinement statistics are listed in Table 1.

N-ColE7/Im7/Ni^{2+} crystallization and data collection

E. coli M15 cells with pQE-70 plasmid were used for expression of the H545E mutant of N-ColE7 and Im7. The mutated N-ColE7/Im7 complex was purified by similar methods described previously for the purification of wild-type N-ColE7/Im7 (Ko et al. 1999). The purified protein complex was dialyzed in 0.1 M Tris-HCl, 1 mM EDTA buffer (pH 8) overnight to remove any associated metal ions. The protein sample was then dialyzed in Mini-Q water followed by dialysis in 2 mM $NiCl_2$ for 10 h. The Ni-bound protein complex was then concentrated to 10 mg/mL in Mini-Q water by VIVASPIN concentrator (VIVASCIENCE).

Crystals of N-ColE7/Im7/Ni^{2+} were grown by a hanging-drop vapor-diffusion method at room temperature, from a droplet consisting of 3 μL of protein solution and 3 μL of reservoir solution (0.3 M phosphate buffer at pH 5.7, 50 mM NaCl, 20% PEG550 MME, and 10% glycerol). Crystals appeared in 1 wk and were flash cooled in liquid nitrogen without addition of cryoprotectant before data collection. Data were collected by a Quantum 4 CCD detector at Taiwan beamline BL12B2 in SPring-8, Japan. The crystals diffracted X-rays to a resolution of 2.0 Å and all the diffraction statistics are listed in Table 1.

N-ColE7/Im7/Ni^{2+} structure determination and refinement

The Ni-bound H545E N-ColE7/Im7 complex crystallized in the space group P21212, isomorphous to the structure of Zn-bound N-ColE7/Im7 (Sui et al. 2002). The structure of N-ColE7/Im7/Ni was refined using the previously determined structure (PDB accession no. 1MZ8) by the program CNS (Brunger et al. 1998). This model was subjected to manual rebuilding with Turbo-Frodo, alternating with torsional angle-simulated annealing, standard positional and individual isotropic B value refinement, and automatic water placement and deletion with the CNS program (Brunger et al. 1998). A Fourier $(2F_o − F_c)$ map of the metal-binding site was calculated at the final stage of refinement. Metal ions and phosphate ions were added into the model before the last cycle of refinement. The final refinement statistics are listed in Table 1. Structural coordinates and diffraction structure factors of N-ColE7/Im7/Ni^{2+} have been deposited in the Protein Data Bank with a RCSB ID code of RCSB032935 and a PDB ID code of 1ZNV.

References

Alatossava, T., Jutte, H., Kuhn, A., and Kellenberger, E. 1985. Manipulation of intracellular magnesium content in polymyxin B nonapeptide-sensitized *Escherichia coli* by lonophore A23187. *J. Bacteriol.* **162:** 413–419.

Blindauer, C.A. and Sandler, P.J. 2005. How to hide zinc in a small protein. *Acc. Chem. Res.* **38:** 62–69.

Brunger, A.T., Adams, P.D., Clore, G.M., DeLano, W.L., Gros, P., Grosse-Kunstleve, R.W., Jiang, J.-S., Kuszewski, J., Nilges, N., Pannu, N.S., et al. 1998. Crystallography and NMR system (CNS): A new software system for macromolecular structure determination. *Acta Cryst.* **D54:** 905–921.

Chak, K.-F., Safo, M.K., Ku, W.-Y., Hsieh, S.-Y., and Yuan, H.S. 1996. The crystal structure of the ImmE7 protein suggests a possible colicin-interacting surface. *Proc. Natl. Acad. Sci.* **93:** 6437–6442.

Cheng, Y.-S., Hsia, K.-C., Doudeva, L.G., Chak, K.-F., and Yuan, H.S. 2002. The crystal structure of the nuclease domain of ColE7 suggests a mechanism for binding to double-stranded DNA by the H-N-H endonucleases. *J. Mol. Biol.* **324:** 227–236.

Chevalier, B.S. and Stoddard, B.L. 2001. Homing endonucleases: Structural and functional insight into the catalysts of intron/intein mobility. *Nucleic Acid Res.* **29:** 3757–3774.

Dudev, T. and Lim, C. 2003. Principles governing Mg, Ca, and Zn binding and selectivity in proteins. *Chem. Rev.* **103:** 773–787.

Flick, K.E., Jurica, M.S., Monnat, R.J., and Stoddard, B.L. 1998. DNA binding and cleavage by the nuclear intron-encoded homing endonuclease I-*Ppo*I. *Nature* **394:** 96–101.

Friedhoff, P., Franke, I., Meiss, G., Wende, W., Krause, K.L., and Pingoud, A. 1999. A similar active site for non-specific and specific endonucleases. *Nat. Struct. Biol.* **6:** 112–113.

Galburt, E.A., Chevalier, B., tang, Jurica, M.S., Flick, K.E., Monnat, R.J., and Stoddard, B.L. 1999. A novel endonuclease mechanism directly visualized for I-*Ppo*I. *Nat. Struct. Biol.* **6:** 1096–1099.

Gorbalenya, A.E. 1994. Self-splicing group I and group II introns encode homologous (putative) DNA endonucleases of a new family. *Protein Sci.* **3:** 1117–1120.

Hsia, K.-C., Chak, K.-F., Liang, P.-H., Cheng, Y.-S., Ku, W.-Y., and Yuan, H.S. 2004. DNA binding and degradation by the HNH endonuclease ColE7. *Structure* **12:** 205–214.

Hsia, K.-C., Li, C.-L., and Yuan, H.S. 2005. Structural and functional insight into the sugar-nonspecific nucleases in host defense. *Curr. Opin. Struct. Biol.* **15:** 126–134.

Jones, S., Heyningen, P.V., Berman, H.M., and Thornton, J.M. 1999. Protein–DNA interactions: A structural analysis. *J. Mol. Biol.* **287:** 877–896.

Keeble, A.H., Hemmings, A.M., James, R., Moore, G.R., and Kleanthous, C. 2002. Multistep binding of transition metals to the H-N-H endonuclease toxin colicin E9. *Biochemistry* **41:** 10234–10244.

Kleanthous, C., Kuhlmann, U.C., Pommer, A.J., Ferguson, N., Radford, S.E., Moore, G.R., James, R., and Hemmings, A.M. 1999. Structural and mechanistic basis of immunity toward endonuclease colicins. *Nat. Struct. Biol.* **6:** 243–252.

Ko, T.-P., Liao, C.-C., Ku, W.-Y., Chak, K.-F., and Yuan, H.S. 1999. The crystal structure of the DNase domain of colicin E7 in complex with its inhibitor Im7 protein. *Structure* **7:** 91–102.

Ku, W.-Y., Liu, Y.-W., Hsu, Y.-C., Liao, C.-C., Liang, P.-H., Yuan, H.S., and Chak, K.-F. 2002. The zinc ion in the HNH motif of the endonuclease domain of colicin E7 is not required for DNA binding but is essential for DNA hydrolysis. *Nucleic Acid Res.* **30:** 1670–1678.

Kuhlmann, U.C., Moore, G.R., James, R., Kleanthous, C., and Hemmings, A.M. 1999. Structural parsimony in endonuclease active site: Should the number of homing endonuclease families be redefined? *FEBS Lett.* **463:** 1–2.

Laity, J.H., Lee, B.M., and Wright, P.E. 2001. Zinc finger proteins: New insights into structural and functional diversity. *Curr. Opin. Struct. Biol.* **11:** 39–46.

Lavery, R. and Sklenar, H. 1988. The definition of generalized helicoidal parameters and of axis curvature for irregular nucleic acids. *J. Biomol. Struct. Dyn.* **6:** 63–91.

Li, C.-L., Hor, L.-I., Chang, Z.-F., Tsai, L.-C., Yang, W.-Z., and Yuan, H.S. 2003. DNA binding and cleavage by the periplasmic nuclease Vvn: A novel structure with a known active site. *EMBO J.* **22:** 4014–4025.

Mate, M.J. and Kleanthous, C. 2004. Structure-based analysis of the metal-dependence mechanism of H-N-H endonucleases. *J. Biol. Chem.* **279:** 34763–34769.

Miller, M.D., Cai, J., and Krause, K.L. 1999. The active site of *Serratia* endonuclease contains a conserved magnesium-water cluster. *J. Mol. Biol.* **288:** 975–987.

Mishra, N.C. 2002. *Nucleases—molecular biology and applications.* John Wiley & Sons, Hoboken, New Jersey.

Nadassy, K., Wodak, S.J., and Janin, J. 1999. Structural features of protein-nucleic acid recognition sites. *Biochemistry* **38:** 1999–2017.

Outten, C.E. and O'Halloran, V. 2001. Femtomolar sensitivity of metalloregulatory proteins controlling zinc homeostasis. *Science* **292:** 2488–2492.

Pommer, A.J., Kuhlmann, U.C., Cooper, A., Hemmings, A.M., Moore, G.R., James, R., and Kleanthous, C. 1999. Homing in on the role of transition metals in the HNH motif of colicin endonuclease. *J. Biol. Chem.* **274:** 27153–27160.

Pommer, A.J., Cal, S., Keeble, A.H., Walker, D., Evans, S.J., Kuhlmann, U.C., Cooper, A., Connolly, B.A., Hemmings, A.M., Moore, G.R., et al. 2001. Mechanism and cleavage specificity of the H-N-H endonuclease colicin E9. *J. Mol. Biol.* **314:** 735–749.

Raaijmakers, H., Vix, O., Toro, I., Golz, S., Kemper, B., and Suck, D. 1999. X-ray structure of T4 endonuclease VII: A DNA junction resolvase with a novel fold and unusual domain-swapped dimer architecture. *EMBO J.* **18:** 1447–1458.

Raines, R.T. 1998. Ribonuclease A. *Chem. Rev.* **98:** 1045–1065.

Shen, B.W., Landthaler, M., Shub, D.A., and Stoddard, B.L. 2004. DNA binding and cleavage by the HNH homing endonuclease I-HmuI. *J. Mol. Biol.* **342:** 43–56.

Shub, D.A., Goodrich-Blair, H., and Eddy, S.R. 1994. Amino acid sequence motif of group I intron endonucleases is conserved in open reading frames of group II introns. *Trends Biochem. Sci.* **19:** 402–404.

Suck, D. 1994. DNA recognition by DNase I. *J. Mol. Recognit.* **7:** 65–70.

Sui, M.-J., Tsai, L.-C., Hsia, K.-C., Doudeva, L.-G., Chak, K.-F., and Yuan, H.S. 2002. Metal ions and phosphate binding in the H-N-H motif: Crystal structures of the nuclease domain of ColE7/Im7 in complex with a phosphate ion and different divalent metal ions. *Protein Sci.* **11:** 2947–2957.

Tottey, S., Harvie, D.R., and Robinson, N.J. 2005. Understanding how cells allocate metals using metal sensors and metallochaperones. *Acc. Chem. Res.* **38:** 775–783.

Travers, A. 2000. Recognition of distorted DNA structures by HMG domains. *Curr. Opin. Struct. Biol.* **10:** 102–109.

van den Bremer, E.T.J., Jiskoot, W., James, R., Moore, G.R., Kleanthous, C., Heck, A.J.R., and Maier, C.S. 2002. Probing metal ion binding and conformational properties of the colicin E9 endonuclease by electrospray ionization time-of-flight mass spectrometry. *Protein Sci.* **11:** 1738–1752.

van den Bremer, E.T.J., Keeble, A.H., Jiskoot, W., Spelbrink, R.J., Maier, C.S., Van Hoek, A., Visser, A.J.W.G., James, R., Moore, G.R., Kleanthous, C., et al. 2004. Distinct conformational stability and functional activity of four highly homologous endonuclease colicins. *Protein Sci.* **13:** 1391–1401.

van den Heuvel, R.H.H., Gato, S., Versluis, C., Gerbaux, P., Kleanthous, C., and Heck, A.J.R. 2005. Real-time monitoring of enzymatic DNA hydrolysis by electrospray ionization mass spectrometry. *Nucleic Acid Res.* **33:** e96.

Walker, D.C., Georgiou, T., Pommer, A.J., Walker, D., Moore, G.R., Kleanthous, C., and James, R. 2002. Mutagenic scan of the H-N-H motif of colicin E9: Implications for the mechanistic enzymology of colicins, homing enzymes and apoptotic endonucleases. *Nucleic Acid Res.* **30:** 3225–3234.

Wittmayer, P.K. and Raines, R.T. 1996. Substrate binding and turnover by the highly specific I-*Ppo*I endonuclease. *Biochemistry* **35:** 1076–1083.